AIP Advances

RESEARCH ARTICLE | AUGUST 21 2023

All-solid-state CW Pr^{3+}:YLF green laser at 522 nm end-pumped by a high-power fiber-coupled 444 nm blue LD module

Fengqin Li ; Jin Chen ; Yupeng Weng

Check for updates

AIP Advances 13, 085323 (2023)
https://doi.org/10.1063/5.0166289

CrossMark

View Online

Export Citation

Articles You May Be Interested In

Ion-pair upconversion pumped laser emission in Er^{3+} ions in YAG, YLF, SrF_2, and CaF_2 crystals

Journal of Applied Physics (September 1988)

Diode-Pumped Yb 3+ :YLF and Yb 3+ : CaF 2 Laser Performance

AIP Conference Proceedings (February 2010)

High-Efficiency Room-Temperature 2.06-μm Laser Using Sensitized Ho^{3+}:YLF

Appl. Phys. Lett. (October 2003)

18 September 2023 08:35:00

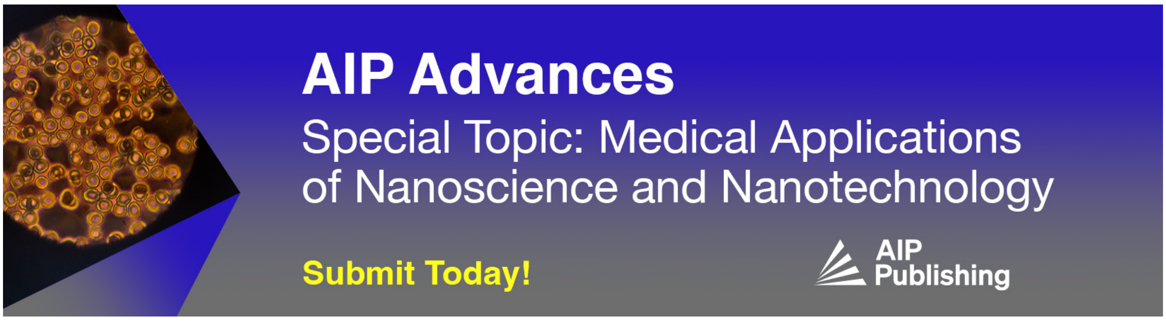

AIP Publishing

All-solid-state CW Pr^{3+}:YLF green laser at 522 nm end-pumped by a high-power fiber-coupled 444 nm blue LD module

Cite as: AIP Advances 13, 085323 (2023); doi: 10.1063/5.0166289
Submitted: 4 July 2023 • Accepted: 30 July 2023 •
Published Online: 21 August 2023

View Online Export Citation CrossMark

Fengqin Li,[1,2,a)] Jin Chen,[1] and Yupeng Weng[1]

AFFILIATIONS

[1] State Key Laboratory of Quantum Optics and Quantum Optics Devices, Institute of Opto-Electronics, Shanxi University, Taiyuan 030006, China
[2] Collaborative Innovation Center of Extreme Optics, Shanxi University, Taiyuan 030006, China

[a)] Author to whom correspondence should be addressed: lfq@sxu.edu.cn

ABSTRACT

Continuous wave (CW) green lasers have a lot of important applications in many fields, including holography, interferometry, atom cooling and trapping, and quantum optics, and they are usually achieved by frequency-doubling 1 μm lasers based on the Nd^{3+} gain media. In this paper, we present an all-solid-state CW green laser with an output wavelength of 522 nm, which was directly attained by employing a Pr^{3+}:YLF crystal pumped with a high-power fiber-coupled blue laser diode (LD) module as the gain medium. Due to the negative thermal lens effect of the Pr^{3+}:YLF crystal, the designed laser resonator had to be lengthened with the increase in the incident pump power. As a result, when a 0.5% doped Pr^{3+}:YLF crystal was employed as the gain medium and the incident pump power was 12 W, the length of the resonator was optimized to 311.3 mm and the maximum output power of 522 nm green laser was up to 886 mW. The obtained conversion efficiency and beam quality M^2 were 11.25% and 1.15, respectively. The long-term power stability within 4.5 h was better than ±1.5% at an output power of 700 mW. The obtained watt-level green laser can also be used to generate high power CW deep UV laser for laser processing of silicon and organic materials, inspection, etc.

© 2023 Author(s). All article content, except where otherwise noted, is licensed under a Creative Commons Attribution (CC BY) license (http://creativecommons.org/licenses/by/4.0/). https://doi.org/10.1063/5.0166289

18 September 2023 08:35:00

I. INTRODUCTION

Continuous wave (CW) green lasers with high power and excellent beam quality have been widely applied in many science and technology fields, such as holography, interferometry, atom cooling and trapping, and quantum optics.[1–3] In addition, they can be extended to deep ultraviolet lasers by nonlinear processes to further satisfy the requirements of semiconductor inspection, grating writing, lithography, and bio-photonics.[4–6] In addition, because the absorption spectrum of a Ti: sapphire crystal is in the blue-green band, green lasers can also be used as pump sources of Ti: sapphire lasers.[7]

Conventionally, CW green lasers were obtained by second harmonic generation (SHG) of all-solid-state near-infrared lasers in the internal or external cavity, which resulted in complicated structures.[8,9] Although the recent progress of green semiconductor lasers can successfully reduce the system complexity, they had a wide linewidth and poor beam quality due to material intrinsic defects, which limited their application in scientific research.[10] Comparatively, trivalent praseodymium (Pr^{3+}) was recognized as one of the most efficient rare-earth ions for direct emission of visible lasers because of its intense radiative transitions in the visible spectra, including 479, 522, 604, 607, 640, 698, and 721 nm.[11] In addition, visible lasers from Pr^{3+} can be easily extended to ultraviolet (UV) lasers only by a single step of SHG, while UV lasers based on infrared lasers near 1 μm required at least two steps of SHG. Among all Pr^{3+}-doped laser crystals, Pr^{3+}:YLF was the most established laser crystal since it exhibited a longer upper state lifetime and smaller photon energy. In the past two decades, thanks to the development of gallium nitride (GaN)-based blue laser diode (LD) near 444 nm and frequency-doubled optically pumped semiconductor laser (OPSL) near 479 nm, which corresponded to the absorption peaks of Pr^{3+}, all-solid-state Pr^{3+}:YLF lasers directly oscillating at red, orange, and blue wavelengths have been realized.[12–14] For green laser, although the emission cross section value of the green transition in Pr^{3+} was relatively weak, which brought about a challenge in the generation of high-power green light, Pr^{3+}-doped crystals provided a new scheme for generating compact and simple green laser. To our knowledge, the highest CW output power of Pr^{3+}:YLF green laser pumped by OPSL was 2.9 W at 523 nm.[15] Although the OPSL pumping source operated with excellent beam quality, it still had a cumbersome structure, leading to relatively large volume and poor reliability of the green laser system. The most efficient and compact pumping system of the Pr^{3+}-doped laser was still the GaN-based LD. In addition, the highest CW output power of 1.7 W at 523 nm has been obtained under a pump power of 4 W of a single-emitter GaN blue LD in 2016.[16] Although the optical conversion efficiency was relatively high, the measured laser beam quality M^2 was about 1.8, which was not perfect for medium pumping power and low thermal effect, and the detailed performance of the laser has not been investigated. In 2018, in order to study the performance of the Pr^{3+}-doped visible laser under the condition of high pumping power, Tanaka *et al.* first demonstrated a 640 nm Pr^{3+}:YLF laser single-end pumped by a high power fiber-coupled blue laser module with an output power of more than 20 W.[17] They successfully suppressed thermal aberration and obtained an output power of 3.4 W at 640 nm with good beam quality. So far, there has been no report on Pr^{3+}-doped green laser operation single end-pumped by a high-power blue laser module.

In this paper, we demonstrated an efficient CW Pr^{3+}:YLF green laser at 522 nm directly single-end pumped by a fiber-coupled LD module with the highest available output power of 12 W at 444 nm. The thermal influence of Pr^{3+}:YLF crystal on the performance of green laser was mainly analyzed to effectively optimize the beam quality and optical conversion efficiency. As a result, when a 0.5% doped Pr^{3+}:YLF crystal was employed as the gain medium and the incident pump power was 12 W, the length of the resonator was optimized to 311.3 mm and the maximum output power of 522 nm green laser was up to 886 mW. The obtained conversion efficiency and beam quality M^2 were 11.25% and 1.15, respectively. The long-term power stability within 4.5 h was better than ±1.5% at an output power of 700 mW. By means of nonlinear frequency doubling technology, the obtained watt-level green laser can be used to generate CW deep UV 261 nm laser with high photon energy, high absorption for many materials, and high scattering intensity. Therefore, it was an important light source for laser processing of silicon, organic materials, and inspection.

II. EXPERIMENTAL DETAILS

The schematic of the LD pumped Pr^{3+}:YLF green laser was shown in Fig. 1. The pumping source was a fiber-coupled LD module with the highest output power of 12 W and a central wavelength of 444 nm. The core diameter and numerical aperture (NA) of the coupling fiber were 200 μm and 0.22, respectively. The measured linewidth and long-time power stability of the LD blue laser were less than 2.6 nm and 0.9% (10 h), respectively. To ensure an output wavelength of 444 nm, the blue LD was mounted on a copper block oven cooled by circulated water and the work temperature was controlled to be 25.00 °C. The pump beam was coupled into the resonator and focused at the center of the gain media by a telescope system consisting of two lenses with the same focal length of 30 mm.

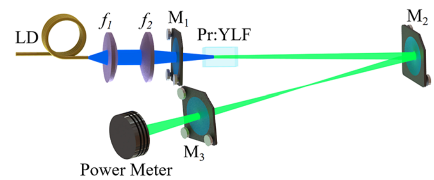

FIG. 1. Schematic of the LD pumped Pr^{3+}:YLF green laser.

A V-folded resonator was constructed by three mirrors (M_1–M_3). The input coupler M_1 was a plane mirror coated with a high reflection (HR) film at 522 ± 20 nm (R > 99.8%) and high transmission (HT) film at 444 nm (T > 95%). Both M_2 and M_3 were plane-concave mirrors with a curvature radius of 100 mm. M_2 was coated with an HR film at 522 ± 20 nm (R > 99.8%). In order to minimize the astigmatism caused by the concave mirror, the folded angle at M_2 was set as small as possible, which was about 4°. The concave of the output coupler M_3 was coated with a fixed transmission film at 522 ± 20 nm and the plane was coated with an HT film at 522 ± 20 nm (T > 95%) to obtain efficient optical conversion. The gain medium was an a-cut Pr:YLF crystal with dimensions of 3 × 3 × 6 mm^3 and a doping concentration of 0.5%, which was placed close to the input mirror M_1 for full absorption of the pump light energy. The front end-face of the crystal was coated with an anti-reflection (AR) film at 444 and 522 nm, and the second end-face was coated with an AR film only at 522 nm. Due to the energy difference between the pump and the oscillating laser photons, the optical pumping process was associated with the generation of heat, leading to a number of undesirable consequences, such as spherical aberration with consequent degradation in laser beam quality, thermal lens, resonator loss, and even rod fracture.[18,19] Hence, mitigating and quantifying the thermal effect of laser crystals have been the focus of the investigation of high-power lasers. In addition, the thermal lens became a critical factor for optimizing the resonator design and scaling the output power of the laser. In the experiment, Pr:YLF crystal was wrapped with an indium foil and placed in a copper oven controlled by a home-made high-precision temperature controller. Based on the thermoelectric refrigeration principle and PID parameter self-tuning control technique, the operating temperature of the Pr:YLF crystal was precisely controlled to be 10.20 °C to dissipate heat as much as possible. In this case, the thermal stress and deformation can be ignored, the thermal effect in the laser crystal primarily depended on the temperature change of the refractive index, and the equivalent thermal lens focal length of the Pr:YLF crystal can be expressed as[20]

$$f = \frac{\pi K_c \omega_p^2}{\xi P_{in} \frac{dn}{dt}} \frac{1}{1 - \exp(-\alpha l)}. \tag{1}$$

The parameters used to calculate the thermal focal length were the thermal conductivity coefficient $K_c = 6$ W m^{-1} K^{-1}, thermo-optical coefficient $dn/dt = -5.2 \times 10^{-6}$ K^{-1}, quantum defect coefficient $\xi = 14.2\%$, $\omega_p = 100$ μm, and absorption coefficient $\alpha = 3.6$ cm^{-1}. Figure 2 showed that the thermal focal length increased with increasing power of the pump blue laser. It can be seen from the figure that the Pr:YLF crystal exhibited strong negative thermal lensing in the case of high pump conditions due to the large negative refractive

18 September 2023 08:35:00

© Author(s) 2023

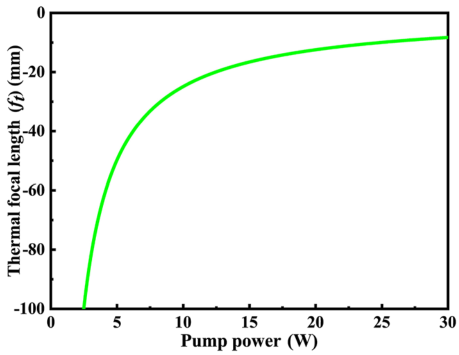

FIG. 2. Thermal focal length of the Pr:YLF crystal as a function of pump power.

index change against temperature. In addition, the negative thermal focal length of the Pr:YLF was very short, only about −35 and −23 mm under pump powers of 7 and 12 W, respectively, making the crystal equivalent to a concave lens with a very short focal length in the optical resonator under high pump power conditions.

Then based on the ABCD transfer matrix and the condition of stable laser operation,[21] the length of the cavity including a negative thermal lens was determined. The distance between M_1 and M_2 was fixed at 140 mm. The function of the beam radius (ω_0) at the Pr:YLF crystal vs the distance (l_2) between M_2 and M_3 under different pump powers was shown in Fig. 3. It can be seen that the scaling of the pump power made the stable region of the laser operation narrower and moved toward a longer distance between M_2 and M_3, which was different from the positive thermal lens as the $Nd:YVO_4$ crystal. In addition, the shorter the distance of l_2, the more sensitive the beam radius at the Pr:YLF crystal was to the increase in pump power. Thus, in the experiment, the output coupling mirror M_3 was fixed on an adjustable three position translation frame to finely change the length of l_2 near 172 mm.

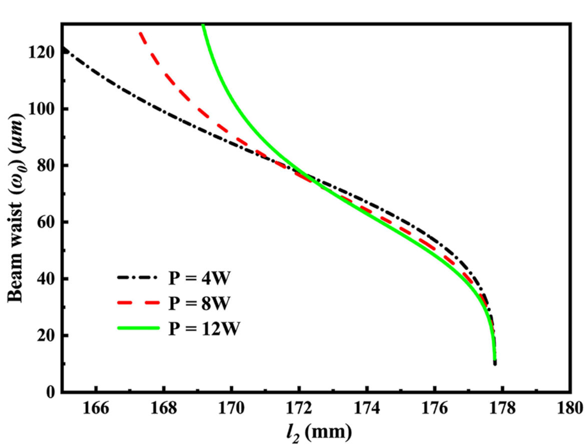

FIG. 3. Beam waist of green laser in the Pr:YLF crystal as a function of l_2.

Furthermore, in order to improve the conversion efficiency, the transmission of the output coupler mirror M_3 was optimized. For end pumping, the laser threshold can be expressed as[22]

$$P_{th} = \frac{1}{\eta_t}\frac{\pi h\nu_p}{2\sigma\tau}(T+L)(\omega_0^2+\omega_p^2)[1-\exp(-\alpha l)]^{-1}, \qquad (2)$$

where $h\nu_p$ was the pumping photon energy, σ was the stimulated emission cross section of the crystal, τ (35.7 μs) was the upper level life of the oscillating laser, T was the transmission of the output coupler, and L was the intracavity loss. In addition, the output power of the laser can be expressed as

$$P_{out} = \frac{T}{T+L} f_{ovl}\eta_t(\nu_0+\nu_p)[1-\exp(-\alpha l)](P_{in}-P_{th}), \qquad (3)$$

where f_{ovl} was the overlapping degree of oscillating light, which was an important factor affecting the beam quality and optical efficiency; η_t (95%) was the power transmission coefficient of the coupling system; and ν_0 and ν_p were the frequency of oscillating and pumping lasers, respectively. Because the emission cross section of the Pr^{3+}:YLF crystal was only 0.3×10^{-19} cm^2 at 522 nm, which was much smaller than that at the peak wavelength of 640 nm (2.2×10^{-19} cm^2), the spot size ω_0 at the Pr:YLF crystal should be designed to be smaller to obtain high output power and lower oscillation threshold of the 522 nm laser. In our experiment, the cavity length l_2 was lengthened to be about 171.3 mm, producing a spot radius (ω_0) of 85 μm in the Pr:YLF crystal to achieve high conversion efficiency and excellent beam quality. Using Eqs. (2) and (3), the transmission of the output coupler M_3 can be optimized to maximize the output power as T_{opt},

$$T_{opt} = \sqrt{\frac{2\sigma\tau\eta_t[1-\exp(-\alpha l)]}{\pi h\nu_p(\omega_0^2+\omega_p^2)}P_{in}L} - L, \qquad (4)$$

where the system linear loss L was given as 2.5%. The relationship between optimal transmission and pumping power with different values of ω_0 was shown in Fig. 4. It can be seen from the figure that the optimal transmissivity of M_3 was about 2.5% at a pump power of 12 W and a spot size (ω_0) of 85 μm.

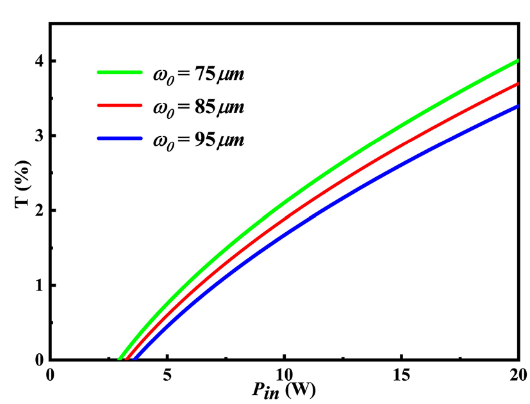

FIG. 4. Relationship between optimal transmission and input power.

18 September 2023 08:35:00

© Author(s) 2023

III. EXPERIMENT RESULTS AND ANALYSES

As a result, efficient generation of green laser with the transverse Gaussian (TEM_{00}) mode was obtained. Figure 5 showed the generated output power of green laser when the transmissions of M_3 were fixed at 1.5%, 2%, and 2.5%. Obviously, the experiment results were almost consistent with the theoretical expectations. When the transmission of M_3 was 1.5% or 2%, the output power of green laser began to decrease if the pump power continued to increase beyond 10 W, which showed slight saturation of the output power. When the transmission was fixed at 2.5%, the maximum output power of 886 mW at 522 nm was obtained under an incident pump power of 12 W and the corresponding conversion efficiency was 11.25%. The pumping threshold power was about 4 W. There were no observed power saturation and crystal fracture. If the input power continued to increase, the output power of the green laser can probably increase. The lower optical conversion efficiency than the results in the literature[17] was believed to be the serious resonator loss caused by the thermal effect under high pump power. Simultaneously, the Gaussian beam profile was measured by a beam quality analyzer (Thorlabs, BP209-VIS), as shown in Fig. 6. Fortunately, the light intensity showed a good TEM_{00} Gaussian distribution, and the measured values of M_x^2 and M_y^2 were both 1.15 at a distance of 300 mm outside mirror M_3. When the output power was 700 mW, the stability within 4.5 h was better than ±1.5%, as shown in Fig. 7.

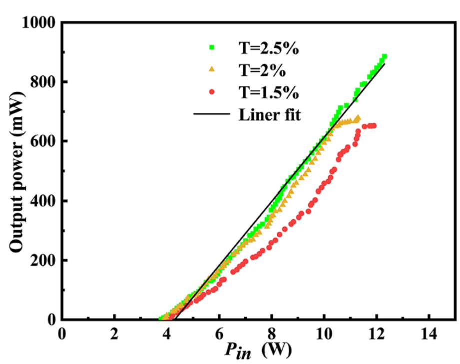

FIG. 5. Output power vs incident power.

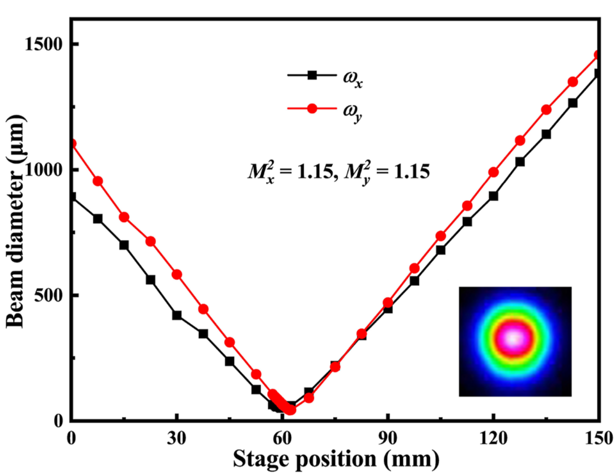

FIG. 6. Measurement results of beam quality.

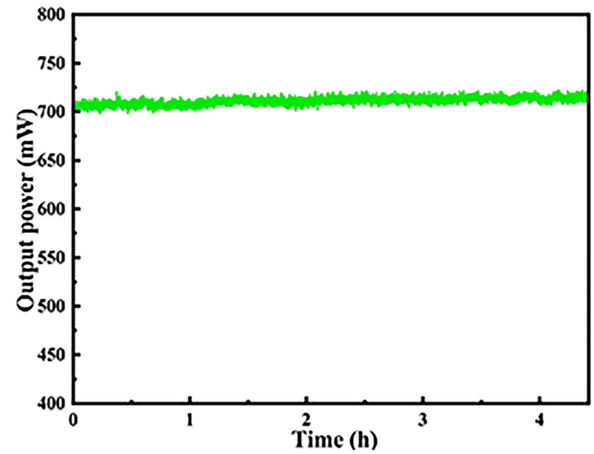

FIG. 7. Long term output power stability of green laser.

IV. CONCLUSION

A 522 nm efficient all-solid-state CW Pr^{3+}:YLF green laser directly pumped by high power with an output fiber-coupled blue laser diode (LD) module was presented. Based on the analysis of the laser crystal thermal effect, the performance of the laser was optimized to effectively improve the optical conversion efficiency and beam quality. By employing a Pr^{3+}:YLF crystal with 0.5% doping concentration as the gain medium, the 522 nm green laser with the highest output power of 886 mW was obtained at a single-end pump power of 12 W. The conversion efficiency and beam quality M^2 were 11.25% and 1.15%, respectively. The stability within 4.5 h was better than ±1.5% at an output power of 700 mW. The laser performance shown in this paper can meet the needs of developing scientific research. In addition, the Pr^{3+}:YLF laser still held potential for power scaling in high power LD pumping by further optimizing the doping concentration of crystal and cavity parameters.

ACKNOWLEDGMENTS

This work was supported by the National Natural Science Foundation of China (Grant Nos. 61975100, 62027821, and 62105192), the Applied Basic Research Project of Shanxi Province (Grant No. 20210302121004), the Key R&D Program of Shanxi Province (Grant No. 202102150101002), the Program for the Innovative Talents of High Education Institutions of Shanxi, the Fund for Shanxi "1331 Project" Key Subjects Construction, and the research project supported by the Shanxi Scholarship Council of China (Grant No. 2022-015).

18 September 2023 08:35:00

© Author(s) 2023

AUTHOR DECLARATIONS

Conflict of Interest

The authors have no conflicts to disclose.

Author Contributions

Fengqin Li: Conceptualization (equal); Data curation (equal); Formal analysis (equal); Investigation (equal); Supervision (equal); Validation (equal); Writing – review & editing (equal). **Jin Chen**: Data curation (equal). **Yupeng Weng**: Data curation (equal).

DATA AVAILABILITY

The data that support the findings of this study are available from the corresponding author upon reasonable request.

REFERENCES

[1] Y. Ruan, Q. Xu, and L. Lin, "Progress in the technology and materials of blue-green lasers," J. Synth. Cryst. **31**(3), 266–276 (2002).

[2] Y. Nakatsu, Y. Nagao, K. Kozuru, T. Hirao, E. Okahisa, S. Masui, T. Yanamoto, and S.-I. Nagahama, "High-efficiency blue and green laser diodes for laser displays," Proc. SPIE **10918**, 109181D (2019).

[3] W. Yang, S. Shi, Y. Wang, W. Ma, Y. Zheng, and K. Peng, "Detection of stably bright squeezed light with the quantum noise reduction of 126 dB by mutually compensating the phase fluctuations," Opt. Lett. **42**(21), 4553–4556 (2017).

[4] A. S. Rao, N. A. Chaitanya, and G. K. Samanta, "High-power, high repetition-rate, ultrafast fibre laser based source of DUV radiation at 266 nm," OSA Continuum **2**(1), 99 (2019).

[5] Z. Fang, Z. Hou, F. Yang, L. Liu, X. Wang, Z. Xu, and C. Chen, "High-efficiency UV generation at 266 nm in a new nonlinear optical crystal $NaSr_3Be_3B_3O_9F_4$," Opt. Express **25**(22), 26500–26507 (2017).

[6] Q. Liu, X. Yan, M. Gong, H. Liu, G. Zhang, and N. Ye, "High-power 266 nm ultraviolet generation in yttrium aluminum borate," Opt. Lett. **36**(14), 2653–2655 (2011).

[7] F. Li, B. Zhao, J. Wei, P. Jin, H. Lu, and K. Peng, "Continuously tunable single-frequency 455 nm blue laser for high-state excitation transition of cesium," Opt. Lett. **44**(15), 3785–3788 (2019).

[8] F. Li, Y. Zheng, and K. Zhang, "All-solid-state high power CW Nd:YVO_4/LBO green laser of TEM_{00} operation," J. Quantum Opt. **12**(3), 176–179 (2006).

[9] Q. Yin, H. Lu, J. Su, and K. Peng, "High power single-frequency and frequency-doubled laser with active compensation for the thermal lens effect of terbium gallium garnet crystal," Opt. Lett. **41**(9), 2033–2036 (2016).

[10] M. Adachi, Y. Yoshizumi, Y. Enya, T. Kyono, T. Sumitomo, S. Tokuyama, S. Takagi, K. Sumiyoshi, N. Saga, T. Ikegami, M. Ueno, K. Katayama, and T. Nakamura, "Low threshold current density inGaN based 520–530 nm green laser diodes on semi-polar {2021} free-standing GaN substrates," Appl. Phys. Express **3**(12), 121001 (2010).

[11] L. Esterowitz, F. J. Bartoli, R. E. Allen, D. E. Wortman, C. A. Morrison, and R. P. Leavitt, "Energy levels and line intensities of Pr^{3+} in LiYF," Phys. Rev. B **19**(12), 6442–6455 (1979).

[12] B. Xu, P. Camy, J. L. Doualan, Z. Cai, and R. Moncorgé, "Visible laser operation of Pr^{3+}-doped fluoride crystals pumped by a 469 nm blue laser," Opt. Express **19**(2), 1191–1197 (2011).

[13] F. Cornacchia, A. Richter, E. Heumann, G. Huber, D. Parisi, and M. Tonelli, "Visible laser emission of solid state pumped $LiLuF_4$:Pr^{3+}," Opt. Express **15**(3), 992–1002 (2007).

[14] M. He, S. Chen, Q. Na, S. Luo, H. Y. ZhuLi, C. Xu, and D. Fan, "Watt-level Pr^{3+}:YLF deep red laser pumped by a fiber-coupled blue LD module or a single-emitter blue LD," Chin. Opt. Lett. **18**(1), 011405 (2020).

[15] P. W. Metz, K. Hasse, D. Parisi, N. O. Hansen, C. Kränkel, M. Tonelli, and G. Huber, "Continuous-wave Pr^{3+}:BaY_2F_8 and Pr^{3+}:$LiYF_4$ in the cyan-blue spectral region," Opt. Lett. **39**(17), 5158–5161 (2014).

[16] S. Luo, X. Yan, Q. Cui, B. Xu, H. Xu, and Z. Cai, "Power scaling of blue-diode-pumped Pr:YLF lasers at 523.0, 604.1, 606.9, 639.4, 697.8 and 720.9 nm," Opt. Commun. **380**, 357–360 (2016).

[17] H. Tanaka, S. Fujita, and F. Kannari, "High-power visibly emitting Pr^{3+}:YLF laser end pumped by single-emitter or fiber-coupled GaN blue laser diodes," Appl. Opt. **57**(21), 5923–5928 (2018).

[18] R. Martinez-Herrero, P. M. Mejias, N. Hodgson, and H. Weber, "Beam-quality changes generated by thermally-induced spherical aberration in laser cavities," IEEE J. Quantum Electron. **31**(12), 2173–2176 (1995).

[19] L. McDonagh, R. Wallenstein, R. Knappe, and A. Nebel, "High-efficiency 60 W TEM_{00} Nd:YVO_4 oscillator pumped at 888 nm," Opt. Lett. **31**(22), 3297–3299 (2006).

[20] Y. Wang, W. Yang, H. Zhou, M. Huo, and Y. Zhen, "Temperature dependence of the fractional thermal load of Nd:YVO_4 at 1064 nm lasing and its influence on laser performance," Opt. Express **21**(15), 18068–18078 (2013).

[21] S. Lee, M. Yun, B. Cha, C. Kim, S. Suk, and H. Kim, "Stability analysis of a diode-pumped, thermal birefringence-compensated two-rod Nd:YAG laser with 770-W output power," Appl. Opt. **41**(27), 5625–5631 (2002).

[22] M. Vainio, J. Peltola, S. Persijn, F. J. M. Harren, and L. Halonen, "Thermal effects in singly resonant continuous-wave optical parametric oscillators," Appl. Phys. B **94**(3), 411–427 (2009).

18 September 2023 08:35:00

© Author(s) 2023